

Quantitative Evaluation of Color Enhancement Methods for Underwater Photogrammetry in Very Shallow Water: a Case Study

Original

Quantitative Evaluation of Color Enhancement Methods for Underwater Photogrammetry in Very Shallow Water: a Case Study / Calantropio, A., Chiabrande, F., Menna, F., Nocerino, E.. - In: INTERNATIONAL ARCHIVES OF THE PHOTOGRAMMETRY, REMOTE SENSING AND SPATIAL INFORMATION SCIENCES. - ISSN 2194-9034. - ELETTRONICO. - X-2-2024:(2024), pp. 25-32. [10.5194/isprs-annals-X-2-2024-25-2024]

Availability:

This version is available at: 11583/2999528 since: 2025-04-25T09:18:16Z

Publisher:

Copernicus Publ.

Published

DOI:10.5194/isprs-annals-X-2-2024-25-2024

Terms of use:

This article is made available under terms and conditions as specified in the corresponding bibliographic description in the repository

Publisher copyright

(Article begins on next page)

Quantitative Evaluation of Color Enhancement Methods for Underwater Photogrammetry in Very Shallow Water: a Case Study

Alessio Calantropio¹ *, Filiberto Chiabrando², Fabio Menna³, Erica Nocerino¹

¹ Department of Humanities and Social Sciences, University of Sassari, Sassari, Italy - (acalantropio, enocerino)@uniss.it

² Department of Architecture and Design, Politecnico di Torino, Torino, Italy - filiberto.chiabrando@polito.it

³ Department of Chemical, Physical, Mathematical and Natural Sciences, University of Sassari, Sassari, Italy - fmenna@uniss.it

Commission II/WG6

Key Words: Underwater photogrammetry, color enhancement, depth maps, color checker, shallow water, 3D metric survey, underwater archaeology, artificial intelligence, deep learning

Abstract:

Underwater photogrammetry is often hampered by chromatic aberration, leading to degraded 2D and 3D products. This study investigates the effectiveness of various color enhancement methods in addressing these challenges. Theoretical considerations indicate that light penetration depth varies inversely with wavelength, causing underwater images to exhibit a blue or green cast with increasing depth. Color enhancement techniques can restore natural colors by compensating for this spectral attenuation. Additionally, scattering, caused by light reflected by particles in the water, can introduce haze into underwater images. Color enhancement can mitigate scatter and improve image clarity. In this contribution, to quantitatively evaluate color enhancement methods, we compare original images with images processed using gray-world assumption methods and physical methods that account for the physical properties of light underwater. Using artificial intelligence (AI) for underwater image color enhancement, a data-driven approach was also employed. These methods were applied to a case study concerning a Roman Navis Lapidaria shipwreck carrying five monumental cipollino marble columns at a depth of 4.5 meters in the Porto Cesareo Marine Protected Area (Italy). These methods were compared quantitatively and qualitatively, and the results are presented and discussed.

1. Introduction

The field of underwater imaging encompasses a diverse range of applications, from underwater surveying and archaeology to marine biology and conservation. Color accuracy and image clarity are paramount for effective data capture and analysis in these domains. Underwater imaging poses significant challenges due to the unique properties of light. Water's selective absorption of light wavelengths contributes to the loss of light wavelength components as it travels through the water column, imparting a distinctive bluish tint to underwater images. Additionally, particles suspended in the water, such as plankton and sediment, scatter light and further contribute to image degradation. These factors make it difficult to capture accurate color reproduction and sharp images underwater. Various techniques have been developed to address these challenges to enhance underwater imaging. These techniques utilize image processing algorithms to post-process underwater images, correcting for color balance, enhancing sharpness, and reducing noise.

1.1 Understanding Color Rendering Underwater

An important factor influencing the survey is the depth in which the assets are located. This is related to a degradation in the visible electromagnetic spectrum, and it is an important aspect of the study and recognition of the materials, both for photographic and photogrammetric purposes. Water absorbs part of the light that passes through it. This absorption is not homogeneous but occurs differently, depending on the mass of water crossed by the light for the various colors. The phenomenon is known precisely

because it occurs selectively on the various colors, called "selective absorption" (Figure 1).

Underwater images are affected by inconsistencies in radiometry due to the optical properties of water. As light travels through water, the intensity of all colors (but significantly higher wavelengths) decreases. This degradation varies depending on the wavelength, the depth of the water, the distance between the camera and the object, and the physical characteristics and conditions of the water at the specific location and time of the image being taken. Water attenuates light as it travels through it, causing the intensity of light to decrease with increasing distance (Jaffe, 1990). Light underwater is attenuated more intensely for longer wavelengths, such as red light, than for shorter wavelengths, such as blue light. This difference in attenuation causes objects to appear bluer or greener as they are photographed from greater depths (Bryson et al., 2016).

As described by Wang et al. (Wang et al., 2019b), UW (underwater) images exhibit a consistent green-bluish color cast attributed to the varying attenuation rates of red, green, and blue light (Wang et al., 2019a). The attenuation of light in water, and consequently the appearance of underwater scenes, is influenced by scattering and absorption processes governed by attenuation coefficients. These coefficients determine how light intensity diminishes with increasing travel distance (Bekerman et al., 2020). In pure water, light absorption occurs primarily through interactions with water molecules and dissolved ions, as suspended particles are absent. (Morel, 1974). Long visible wavelengths such as red are absorbed first, followed by green and

* Corresponding author

blue. As a result, only a fraction of the sunlight reaching the water's surface penetrates depths beyond 100 meters (Menna et al., 2018).

Another factor that should not be underestimated is the presence of materials in the water: for example, if we consider the delta of a river or a lagoon environment (Costa, 2022), the suspended sand and clay particles may give the water a turbid appearance and a color tending to brown. The presence of phytoplankton is another cause of color distortion in underwater environments; in fact, it absorbs blue and red, resulting in a reflection of green. In practice, where there is water with phytoplankton, its color will be more green than blue. Scientists exploit this information to assess the distribution and location of phytoplankton worldwide.

Another factor to be considered is the depth of the bottom. If we are in the middle of the ocean, the light will not be able to penetrate for more than a few hundred meters, so - in other words - we will not have any reflection of the bottom, and we will see the water of a dark and intense blue. If, on the other hand, we are close to the coast, we will see the water of a brilliant blue turquoise due in part to the reflection of the seabed.

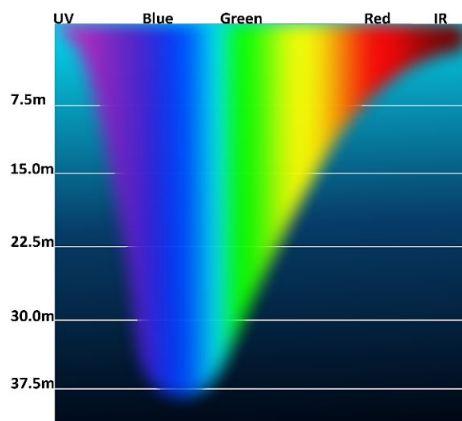


Figure 1. This graph approximates how deep specific wavelengths (and related colors) can penetrate a water column. Source: Wikimedia Commons, Author: Tomemorris, License: CC-BY-SA-4.0

2. State of the art on Color Enhancement Methods

Underwater image color enhancement is an essential area of research for disciplines such as underwater archaeology and marine biology. Domain experts and scientists need images with colors that are consistent with the real-world scene. Automatic and semi-automatic color enhancement methods and algorithms have been developed to meet this need and are mainly used in the pre- or post-processing phases of photogrammetry (Akkaynak & Treibitz, 2019; Bianco et al., 2015; Bryson et al., 2013, 2016; Roznere & Li, 2019; Wu et al., 2017). The literature contains different methods, which can be grouped based on the approaches used to perform the task of underwater image color enhancement (Grimaldi et al., 2023); this section will provide an overview of these methods and their applicability to the research topic.

2.1 Statistical and Mathematical Methods

These methods use statistical models to estimate the degradation factors, such as light attenuation, scattering, and noise, and then use these estimates to restore the image. Water absorption and scattering coefficients have been a subject of ongoing scientific inquiry for many years. In 1951, Jerlov classified water bodies

into three oceanic and five coastal types based on these coefficients (Jerlov et al., 1951). Since then, various methods have been developed to determine the inherent optical properties associated with each Jerlov water type (Solonenko & Mobley, 2015). A mathematical model for spectral analysis of water characteristics was proposed by Blasinski et al. (2014). This model describes the inherent optical properties of water, which can then be used for underwater image color enhancement (Akkaynak et al., 2017). A simple fusion-based approach for enhancing underwater images was proposed by (Ancuti et al., 2012). This method uses a single input image and blends multiple well-known filters to improve image quality. The authors showed that this method effectively improves underwater footage of dynamic scenes.

Some studies have attempted to address UW color attenuation using specialized calibrated equipment and prior knowledge gained from measurements, such as surface reflectance, water attenuation coefficient, and image intensity reference values obtained from calibrated color charts and spectrometers. In 2021 (Vlachos et al., 2022) proposed a mathematical method to color-correct underwater images by modeling light backscattering and absorption variation according to the distance of the surveyed object.

2.2 Heuristic methods - the Gray-world assumption

The gray-world assumption is a well-known approach proposed by Buchsbaum (1980). In its simplest version, it assumes that the information in the average of each channel of the image is the representative gray level. In other words, the average of the captured image should be gray (achromatic). These methods have the advantage of working with any datasets without considering any physical or geometric information, therefore applying enhancements that work only in very generic conditions that mainly differ from real-world applications. Several algorithms that include the gray world assumption have been developed, such as Lab Color Enhancement (Bianco et al., 2015), Contrast Limited Automatic Histogram Equalization (CLAHE) (Pizer et al., 1987; Zuiderveld, 1994), etc, to correct the colors of UW imagery, each with its strengths and weaknesses. In digital photography, the "white balance" process allows the camera to interpret the colors appropriately by eliminating the chromatic dominants due to the light that, instead of white, can be colored. White balance eliminates this effect by returning more natural colors, which cannot happen using film. Compared to traditional film photography, the advantage of digital images is that they automatically correct the colors and give them a more similar aspect to the real one. Some digital camera models are provided with "Underwater" acquisition modes that automatically compensate for this issue. However, there are some limits: the camera can reduce the intensity of a chromatic component, for example, blue, if this predominates over the others, but certainly cannot create red where it is absent. This first problem can be partially solved by using the flash. Its white light allows it to revive even the duller colors, but only at a certain distance. What happens with sunlight also happens with a flashlight; as said earlier, colors are absorbed as a function of the amount of water the light passes through; it does not matter which direction the light comes from; what matters is the distance the light travels underwater. A significant drawback of automatic white balance methods is that their effectiveness relies heavily on the color scheme of the scene, as they calculate the average color for the overall view.

A first proposal for color enhancement of UW images using the CIE 1976 Lab color space (a color space defined by the

International Commission on Illumination that expresses color as three values: L for perceptual lightness and a and b for the four unique colors of human vision) is presented in (Bianco et al., 2015). This method white balances the chromatic components and performs histogram cut-off and stretching of the luminance component to increase image contrast. The method performs effectively under a gray-world assumption and uniform scene illumination, appropriate for close-range downward acquisitions such as seabed mapping or underwater photography and in conditions with minimal lighting variations. (Bryson et al., 2013) proposed an automated underwater image color enhancement method using a gray-world color distribution. This means that surface reflectance has a gray-scale distribution independent of scene geometry. This approach is beneficial for imaging large-scale biological environments, where using color charts is not always possible.

2.3 Physically based methods

These methods consider the physical properties of light underwater, such as attenuation and scattering. They can provide highly accurate results but require additional information about the underwater environment, such as lighting conditions, depths, distances between the camera and objects, and water properties, which may only sometimes be available or require expensive equipment or complex calculations. Akkaynak & Treibitz (2018) proposed a revised underwater image formation model. They derived the physically valid space of backscatter using oceanographic measurements and validated their model using in situ underwater experiments. The revised model is more physically accurate than the current one but contains more parameters, which can be challenging. However, the researchers also implemented a pipeline called Sea-thru (Akkaynak & Treibitz, 2019) that uses the revised model to correct the colors of underwater images.

2.4 Artificial intelligence methods

Artificial intelligence-based methods have shown promising results in enhancing underwater images by learning from a large annotated dataset. (Levy et al., 2023) presented SeaThru-NeRF¹, a new rendering model for NeRFs in scattering media, which is based on the SeaThru image formation model and suggests a suitable architecture for learning both scene information and medium parameters. In 2023, Jamieson et al. proposed DeepSeeColor² (Jamieson et al., 2023). This novel algorithm combines a state-of-the-art underwater image formation model with the computational efficiency of deep learning frameworks. In their experiments, the authors show that DeepSeeColor offers comparable performance to the popular "Sea-Thru" algorithm while being able to rapidly process images at up to 60Hz, thus making it suitable for use onboard AUVs as a preprocessing step to enable more robust vision-based behaviors.

3. Evaluation of Color Enhancement Methods

In this work, we processed the acquired images with different color enhancement methods:

- A. Original images: exported in .jpg format starting from the camera raw format.
- B. UW camera setting: The camera automatically enhances the color on the fly to acquire the images.

- C. White balance: The process of adjusting the colors in an image to make a white object appear white under any light source. Underwater, the light source is different from on land, so it is important to white-balance underwater images to achieve accurate colors. White balance can be achieved using various methods, such as a white or gray balance card.
- D. The Lab algorithm: based on gray-world and uniform illumination assumptions applied in the CIELAB color space (Fairchild, 2010). Color enhancement is performed by white balancing of chromatic components (α and β), while the luminance component l is processed to improve the image contrast. (Bianco et al., 2015)
- E. The Sea-thru algorithm (Akkaynak & Treibitz, 2019) is a physics-based algorithm using the Akkaynak-Treibitz underwater image formation model. The authors state that their model does not use neural networks and was not trained on any dataset. It works without a color chart or any information about the optical qualities or depth of the water body.
- F. The DeepSeeColor algorithm (Jamieson et al., 2023) is a free, open-source, AI-powered color enhancement algorithm specifically designed for underwater images. DeepSeeColor uses a deep learning model to analyze the image and adjust the colors to produce a more natural-looking result.

Methods A and B are automatically applied during the image acquisition phase. In contrast, the authors of this paper have applied C, D, and F - using the standard settings of iterations and learning rate presented in (Jamieson et al., 2023). Method E has been applied as a courtesy by one of the respective creators of the algorithm. The images processed with the described approaches are compared following the method presented in section 3.2.

3.1 Dataset acquisition and processing

The dataset employed for the comparison and evaluation of the above color enhancement methods was acquired over the shipwreck of a Roman Navis Lapidaria, with a cargo of five monumental cipollino marble columns and one block from the quarries of Karystos in Evia, Greece, 8.5-8.8 meters long, with a total weight of 78 tons, lies 4.5 meters deep, located in the AMP of Porto Cesareo (Italy). The ship ran aground due to its draft (3 meters) being greater than the depth at the site, considering that the sea level was then approximately 3 m lower than today. In the framework of this research, a compact underwater camera (Olympus Stylus TG-6) and a color calibration chart (ColorChecker® Classic | X-Rite³) were used (Figure 2).



Figure 2. The Olympus Stylus TG-6 and the ColorChecker® Classic | X-Rite calibration chart are employed in the framework of this research.

X-Rite manufactures two versions of the ColorChecker test chart with slightly different reference values. The reference values of

³ Since the 1st of July 2021, X-Rite Incorporated and Calibrite announced their partnership to transition the X-Rite photo and video portfolio to Calibrite.

¹ https://github.com/deborahLevy130/seathru_NeRF

² <https://github.com/warplab/DeepSeeColor>

the chart used in this research match the "After November 2014" version. The dataset was recorded under natural light at a constant depth of about 3m and a camera-to-object distance of about 1,5 m. It comprises 353 raw files converted to .jpg files. The images were processed through a standard self-calibration bundle adjustment based on a structure-from-motion algorithm followed by multi-view stereo in Agisoft Metashape v. 1.7.1. The corresponding depth map was estimated for each image within the photogrammetric process.

3.2 Color enhancement and analysis

Since only one color chart was deployed in the test site, the analysis refers to the same image after applying the different color enhancement methods. The analysis was performed in Matlab: the RGB values were estimated by applying a median filter to each of the 24 patches of the color chart and their Euclidean distances from reference values computed (see Table 1). ΔE represents the Euclidean distance between the measured and reference colors: colors considered more accurate correspond to smaller ΔE values.

As the RGB colorspace is non-perceptually uniform, the same analysis in the CIELAB color space has been performed to provide a better perceptually uniform and standardized comparison (Table 2). In this case, reference colors are within the CIE 1976 Lab color space. All ΔE formulae are designed initially

to have a difference of 1.0, standing for a JND (Just Noticeable Difference), intended as the amount that a color must be changed for a difference to be noticeable to the human eye (Thomas et al., 2013). Specifically for the CIE 1976 Lab color space—adopted in the framework of this research—an $\Delta E \approx 2,3$ corresponds to a JND (Sharma & Bala, 2017).

Figure 4 and Figure 5 display the color accuracy measurements for each of the employed methods, as described in Section 3. Each small square color patch represents the color as measured, while the thick surrounding border indicates the color reference for that specific region of interest (ROI).

On the following pages, the diagrams on the right-hand side depict the placement of measured and reference colors within the CIE 1976 Lab color space on a chromaticity diagram. Red circles represent the color reference, while green circles indicate the measured colors of each color patch. The chromaticity diagram accounts not for color brightness but only for the α and β components. ROIs with a shorter distance between the reference and measured points exhibit smaller chromatic differences, potentially contributing to a lower ΔE value. However, brightness also influences the ΔE value. To provide a comprehensive comparative analysis, the color enhancement methods were applied to the entire dataset, and six orthophotos were created to provide a qualitative comparison (Figure 6).

| ΔE (RGB) | | Color enhancement methods | | | | | |
|-----------------------------|--------------|---------------------------|----|-----|----|-----|-----|
| ROI | Color | A | B | C | D | E | F |
| 1 | DarkSkin | 52 | 63 | 47 | 32 | 25 | 24 |
| 2 | LightSkin | 87 | 81 | 63 | 67 | 101 | 149 |
| 3 | BlueSky | 83 | 57 | 70 | 43 | 132 | 146 |
| 4 | Foliage | 60 | 51 | 41 | 33 | 35 | 83 |
| 5 | BlueFlower | 80 | 53 | 59 | 42 | 138 | 144 |
| 6 | BluishGreen | 78 | 61 | 71 | 86 | 131 | 142 |
| 7 | Orange | 60 | 81 | 49 | 52 | 71 | 32 |
| 8 | PurplishBlue | 88 | 59 | 84 | 36 | 110 | 93 |
| 9 | ModerateRed | 55 | 77 | 43 | 56 | 84 | 86 |
| 10 | Purple | 54 | 53 | 36 | 28 | 102 | 94 |
| 11 | YellowGreen | 69 | 59 | 60 | 66 | 88 | 147 |
| 12 | OrangeYellow | 82 | 78 | 61 | 68 | 44 | 115 |
| 13 | Blue | 104 | 79 | 104 | 39 | 117 | 119 |
| 14 | Green | 82 | 68 | 96 | 85 | 83 | 79 |
| 15 | Red | 49 | 72 | 41 | 61 | 62 | 71 |
| 16 | Yellow | 103 | 91 | 89 | 84 | 56 | 92 |
| 17 | Magenta | 72 | 81 | 56 | 59 | 98 | 132 |
| 18 | Cyan | 78 | 55 | 89 | 82 | 88 | 141 |
| 19 | White | 57 | 45 | 26 | 14 | 28 | 25 |
| 20 | Neutral8 | 65 | 37 | 58 | 31 | 77 | 78 |
| 21 | Neutral6,5 | 75 | 51 | 75 | 40 | 92 | 114 |
| 22 | Neutral5 | 72 | 61 | 62 | 38 | 61 | 120 |
| 23 | Neutral3,5 | 61 | 52 | 46 | 21 | 50 | 74 |
| 24 | Black | 43 | 40 | 25 | 11 | 77 | 58 |
| $\Delta E \bar{X}$ All ROIs | | 71 | 63 | 60 | 49 | 81 | 98 |

Table 1. The table shows the Euclidean distance (RGB color space) between the reference color chart and the different color enhancement methods adopted - A) Original images; B) UW camera setting; C) White balance; D) Lab algorithm; E) Sea-thru algorithm; F) DeepSeeColor algorithm - and the average Euclidean distance for all the 24 patches.

| ΔE (CIELAB) | | Color enhancement methods | | | | | |
|-----------------------------|--------------|---------------------------|------|------|------|------|------|
| ROI | Color | A | B | C | D | E | F |
| 1 | DarkSkin | 18,3 | 21,2 | 14,0 | 14,3 | 15,1 | 17,3 |
| 2 | LightSkin | 35,9 | 32,9 | 25,7 | 25,8 | 28,0 | 36,5 |
| 3 | BlueSky | 29,7 | 18,5 | 26,0 | 10,7 | 48,0 | 34,1 |
| 4 | Foliage | 25,2 | 19,0 | 15,9 | 14,9 | 23,4 | 21,1 |
| 5 | BlueFlower | 27,0 | 17,1 | 20,6 | 13,3 | 47,7 | 36,8 |
| 6 | BluishGreen | 31,5 | 22,9 | 29,9 | 22,6 | 28,4 | 28,4 |
| 7 | Orange | 25,8 | 34,7 | 20,1 | 24,7 | 28,7 | 16,3 |
| 8 | PurplishBlue | 27,5 | 18,4 | 24,7 | 9,7 | 48,8 | 40,4 |
| 9 | ModerateRed | 31,8 | 40,1 | 22,7 | 32,4 | 35,6 | 31,9 |
| 10 | Purple | 26,7 | 24,1 | 18,4 | 13,1 | 55,1 | 55,6 |
| 11 | YellowGreen | 28,1 | 23,0 | 23,7 | 27,2 | 34,7 | 29,8 |
| 12 | OrangeYellow | 39,8 | 37,3 | 29,1 | 32,6 | 17,7 | 41,0 |
| 13 | Blue | 34,8 | 25,2 | 31,6 | 10,8 | 74,5 | 70,3 |
| 14 | Green | 27,5 | 17,9 | 24,2 | 24,4 | 50,5 | 21,8 |
| 15 | Red | 30,0 | 39,9 | 19,9 | 35,6 | 14,5 | 29,1 |
| 16 | Yellow | 40,2 | 34,9 | 30,9 | 31,8 | 25,2 | 23,6 |
| 17 | Magenta | 34,3 | 37,7 | 25,8 | 29,7 | 60,0 | 39,3 |
| 18 | Cyan | 28,1 | 17,8 | 26,0 | 16,0 | 36,3 | 37,8 |
| 19 | White | 22,0 | 17,8 | 12,5 | 9,3 | 5,7 | 5,9 |
| 20 | Neutral8 | 27,5 | 17,0 | 19,3 | 10,4 | 18,3 | 17,8 |
| 21 | Neutral6,5 | 31,0 | 20,5 | 23,2 | 12,8 | 31,0 | 28,2 |
| 22 | Neutral5 | 29,6 | 22,4 | 22,1 | 13,0 | 25,0 | 38,2 |
| 23 | Neutral3,5 | 26,4 | 20,5 | 19,6 | 9,4 | 26,7 | 34,5 |
| 24 | Black | 20,4 | 14,7 | 13,4 | 5,7 | 20,2 | 28,7 |
| $\Delta E \bar{X}$ All ROIs | | 29,1 | 24,8 | 22,5 | 18,8 | 33,3 | 31,9 |

Table 2. The table shows the Euclidean distance (CIELAB color space) between the reference color chart and the different color enhancement methods adopted - A) Original images; B) UW camera setting; C) White balance; D) Lab algorithm; E) Sea-thru algorithm; F) DeepSeeColor algorithm - and the average Euclidean distance for all the 24 patches.

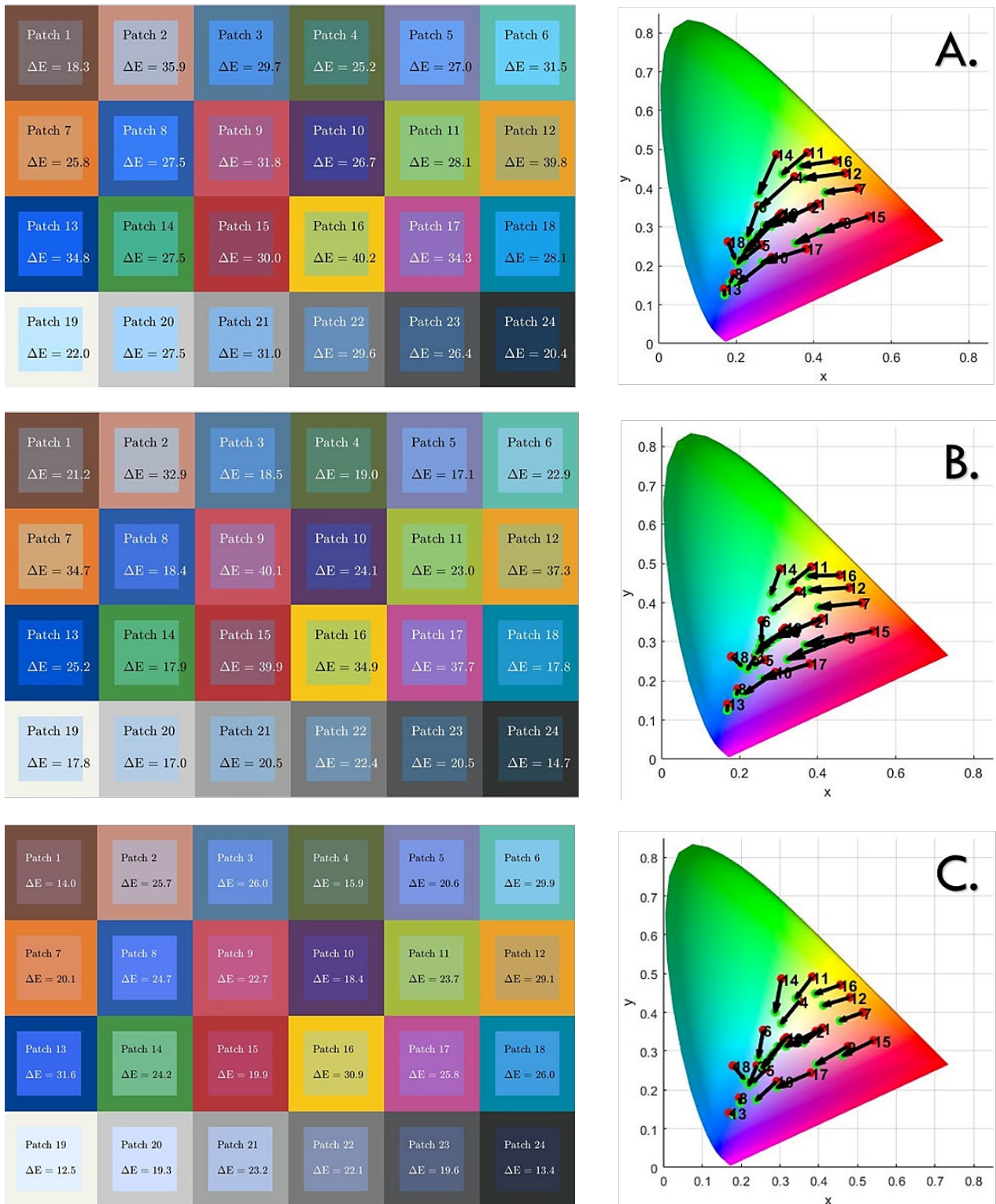


Figure 4. Color accuracy measurements for A) Original images, B) UW camera setting, and C) White balance. On the right, each square color patch is the measured color, and the thick surrounding border is the reference color for that ROI. The diagram on the right shows the measured and reference colors in the CIE 1976 L*a*b* color space on a chromaticity diagram. Red circles indicate the reference color. Green circles indicate the measured color of each color patch. The chromaticity diagram does not portray the brightness of color, but only α and β components.

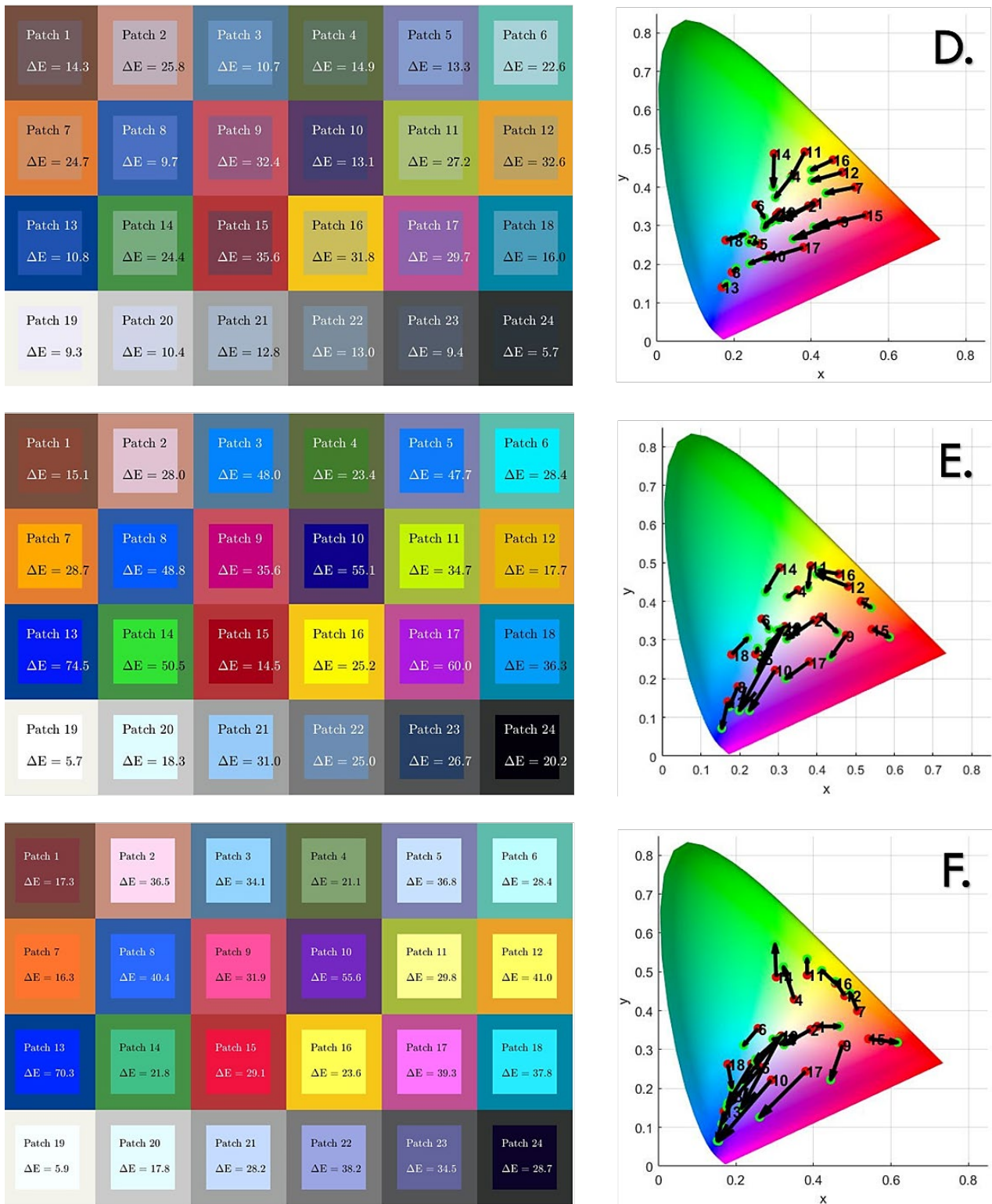


Figure 5. Color accuracy measurements for D) Lab algorithm, E) Sea-thru algorithm, and F) DeepSeeColor algorithm. On the right, each square color patch is the measured color, and the thick surrounding border is the reference color for that ROI. The diagram on the right shows the measured and reference colors in the CIE 1976 L*a*b* color space on a chromaticity diagram. Red circles indicate the reference color. Green circles indicate the measured color of each color patch. The chromaticity diagram does not portray the brightness of color, but only α and β components.

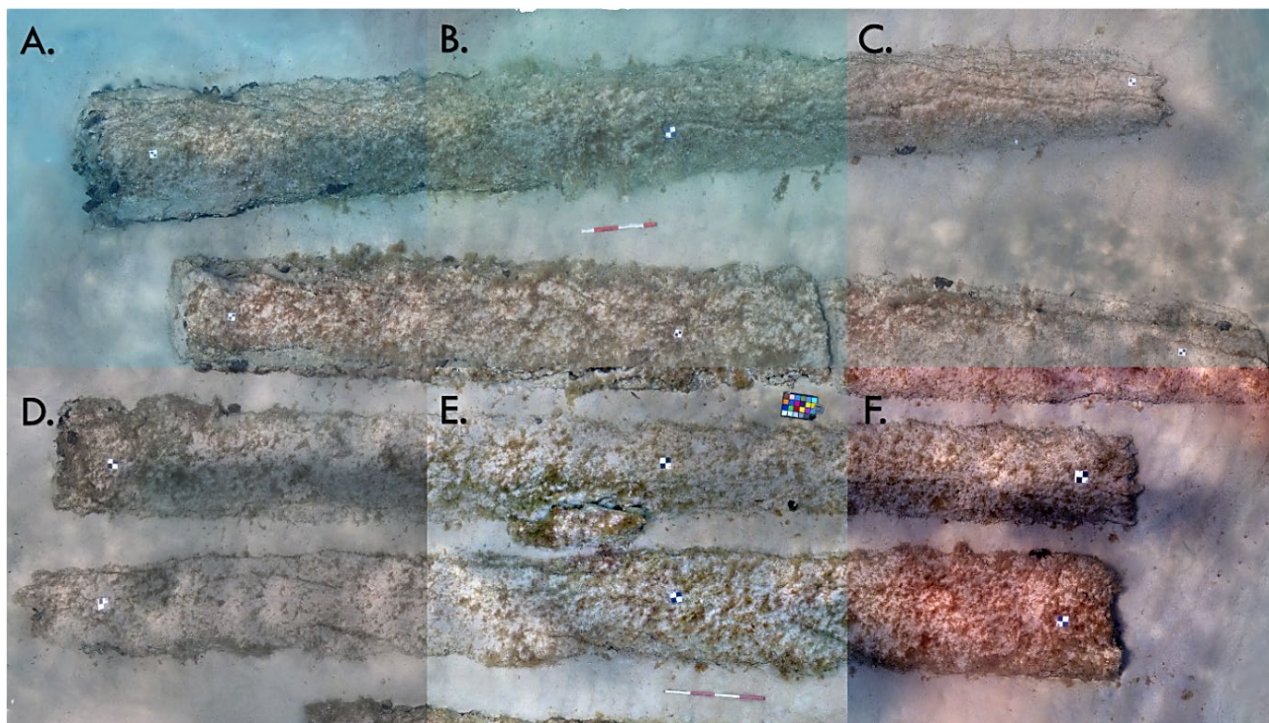


Figure 6. Orthoimages of the cargo of the Navis Lapidaria of AMP Porto Cesareo, A) Original images; B) UW camera setting; C) White balance; D) Lab algorithm; (E) Sea-thru algorithm; F) DeepSeeColor algorithm.

4. Discussions and Conclusions

An evaluation of color enhancement techniques for underwater images was conducted using a dataset of underwater images captured in shallow depths. The evaluation compared original images acquired with the digital camera, together with the automatically on-the-fly color-corrected version (UW camera setting), two traditional methods (white balancing and CIE 1976 Lab color space conversion), one AI-based approach (DeepSeeColor), and a physical model approach (Sea-thru). The results showed that traditional methods performed better than AI-based methods in terms of color accuracy and realism. In the evaluation, white balancing and CIE 1976 Lab color space conversion consistently produced images with more natural colors and better overall quality than AI-based and physical-based methods. This suggests that traditional methods can still be valuable for underwater image enhancement, at least when applied in shallow waters.

Additionally, the evaluation found that the tested AI-based method can introduce artifacts or oversaturate colors, resulting in less realistic images than those produced with traditional methods. It can also not effectively handle some specific challenges of underwater photography, such as the presence of backscatter and caustics. This, however, is an expected outcome since the specific algorithm is tailored for higher depths and different sensors and acquisition configurations than the ones depicted in this research. To the authors' knowledge, a specific AI-based color enhancement method for very shallow water conditions (where there could be more phenomena to consider, such as caustics) is still missing. The evaluation used a limited dataset of underwater images captured in shallow depths. More extensive testing is needed to evaluate the performance of different color enhancement methods across a broader range of conditions and depths.

Despite the advances in underwater image enhancement techniques, achieving perfect color fidelity remains challenging. Traditional methods such as white balancing and CIE 1976 Lab color space conversion may still be effective for correcting color casts and enhancing overall image quality, especially in shallow depths. One important strength of these methods is that they are free, open source, and can be applied by non-specialized operators without additional effort. Ongoing research and development in this field will continue to improve the quality of underwater images; in the following research, the author foresees considering variations in the accuracy of geometric reconstruction when color enhancement methods are applied and including diverse scenes and different depths, allowing for better models' evaluation and enabling more effective data capture and analysis for various applications.

Acknowledgments

We thank Andrea Lingua, Paolo Maschio, and Erica Forti for the technical support during the data acquisition phase, Rita Auriemma, Antonella Antonazzo, and Luigi Coluccia for supporting underwater archaeological investigations. Thanks also to Mino Buccolieri and the authority of Porto Cesareo Marine Protected Area. Many thanks to Derya Akkaynak for her availability to test her algorithm and color-correct our dataset. The authors wish to thank the DIRECT team of Politecnico di Torino for the economic and logistic support. This contribution was realised within the framework of the UnderwaterMuse project, and within the framework of the project MANATEE - Monitoring and mApping of mariNe hABitat with inTegrated gEomatics technologiEs (J53D23002570001) PRIN 2022-2024 project, funded by the European Union, Next Generation EU.

References

Akkaynak, D., & Treibitz, T. (2018). A Revised Underwater Image Formation Model. *Proceedings of the IEEE Computer*

- Society Conference on Computer Vision and Pattern Recognition*, 6723–6732. <https://doi.org/10.1109/CVPR.2018.00703>
- Akkaynak, D., & Treibitz, T. (2019). Sea-THRU: A method for removing water from underwater images. *Proceedings of the IEEE Computer Society Conference on Computer Vision and Pattern Recognition*, 2019-June, 1682–1691. <https://doi.org/10.1109/CVPR.2019.00178>
- Akkaynak, D., Treibitz, T., Shlesinger, T., Tamir, R., Loya, Y., & Iluz, D. (2017). What is the space of attenuation coefficients in underwater computer vision? *Proceedings - 30th IEEE Conference on Computer Vision and Pattern Recognition, CVPR 2017*, 2017-Janua, 568–577. <https://doi.org/10.1109/CVPR.2017.68>
- Ancuti, C., Ancuti, C. O., Haber, T., & Bekaert, P. (2012). Enhancing underwater images and videos by fusion. *Proceedings of the IEEE Computer Society Conference on Computer Vision and Pattern Recognition*, 81–88. <https://doi.org/10.1109/CVPR.2012.6247661>
- Bekerman, Y., Avidan, S., & Treibitz, T. (2020). *Unveiling Optical Properties in Underwater Images*. 1–12. <https://doi.org/10.1109/iccp48838.2020.9105267>
- Bianco, G., Muzzupappa, M., Bruno, F., Garcia, R., & Neumann, L. (2015). A new color correction method for underwater imaging. *International Archives of the Photogrammetry, Remote Sensing and Spatial Information Sciences - ISPRS Archives*, 40(5W5), 25–32. <https://doi.org/10.5194/isprsarchives-XL-5-W5-25-2015>
- Blasinski, H., Breneman IV, J., & Farrell, J. (2014). A MODEL FOR ESTIMATING SPECTRAL PROPERTIES OF WATER FROM RGB IMAGES. *International Conference on Image Processing (ICIP)*, 2, 610–614.
- Bryson, M., Johnson-Roberson, M., Pizarro, O., & Williams, S. B. (2013). Colour-consistent structure-from-motion models using underwater imagery. *Robotics: Science and Systems*, 8, 33–40. <https://doi.org/10.7551/mitpress/9816.003.0010>
- Bryson, M., Johnson-Roberson, M., Pizarro, O., & Williams, S. B. (2016). True Color Correction of Autonomous Underwater Vehicle Imagery. *Journal of Field Robotics*, 33(6), 853–874. <https://doi.org/10.1002/rob.21638>
- Costa, E. (2022). Survey and photogrammetry in underwater archaeological contexts at low visibility in the Venice lagoon. *Digital Applications in Archaeology and Cultural Heritage*, 24, e00215. <https://doi.org/10.1016/j.daach.2022.e00215>
- Fairchild, M. D. (2010). Color appearance models and complex visual stimuli. *Journal of Dentistry*, 38, e25–e33. <https://doi.org/10.1016/j.jdent.2010.05.008>
- Grimaldi, M., Nakath, D., She, M., & Köser, K. (2023). Investigation of the Challenges of Underwater-Visual-Monocular-SLAM. *ISPRS Annals of the Photogrammetry, Remote Sensing and Spatial Information Sciences*, X-1/W1-2023, 1113–1121. <https://doi.org/10.5194/isprs-annals-X-1-W1-2023-1113-2023>
- Jaffe, J. S. (1990). Computer modeling and the design of optimal underwater imaging systems. *IEEE Journal of Oceanic Engineering*, 15(2), 101–111. <https://doi.org/10.1109/48.50695>
- Jamieson, S., How, J. P., & Girdhar, Y. (2023). *DeepSeeColor: Realtime Adaptive Color Correction for Autonomous Underwater Vehicles via Deep Learning Methods* (arXiv:2303.04025). <https://doi.org/10.48550/arXiv.2303.04025>
- Jerlov, N. G., Koczy, F. F., & (Schooner), A. (1951). *Photographic Measurements of Daylight in Deep Water*. Elanders boktr.
- Levy, D., Peleg, A., Pearl, N., Rosenbaum, D., Akkaynak, D., Korman, S., & Treibitz, T. (2023). *SeaThru-NeRF: Neural Radiance Fields in Scattering Media* (arXiv:2304.07743). <https://doi.org/10.48550/arXiv.2304.07743>
- Menna, F., Agrafiotis, P., & Georgopoulos, A. (2018). State of the art and applications in archaeological underwater 3D recording and mapping. *Journal of Cultural Heritage*, 33, 231–248. <https://doi.org/10.1016/j.culher.2018.02.017>
- Morel, A. (1974). *Optical properties of pure water and pure sea water*.
- Roznere, M., & Li, A. Q. (2019). *Real-time Model-based Image Color Correction for Underwater Robots*.
- Sharma, G., & Bala, R. (2017). *Digital Color Imaging Handbook*. CRC Press.
- Solonenko, M. G., & Mobley, C. D. (2015). Inherent optical properties of Jerlov water types. *Applied Optics*, 54(17), 5392. <https://doi.org/10.1364/ao.54.005392>
- Thomas, J.-B., Colantoni, P., & Trémeau, A. (2013). On the Uniform Sampling of CIELAB Color Space and the Number of Discernible Colors. In S. Tominaga, R. Schettini, & A. Trémeau (A c. Di), *Computational Color Imaging* (pp. 53–67). Springer. https://doi.org/10.1007/978-3-642-36700-7_5
- Vlachos, M., Calantropio, A., Skarlatos, D., & Chiabrando, F. (2022). MODELLING COLOUR ABSORPTION OF UNDERWATER IMAGES USING SFM-MVS GENERATED DEPTH MAPS. *The International Archives of Photogrammetry, Remote Sensing and Spatial Information Sciences*, 43, 959–966.
- Wang, Y., Song, W., Fortino, G., Qi, L. Z., Zhang, W., & Liotta, A. (2019a). An Experimental-Based Review of Image Enhancement and Image Restoration Methods for Underwater Imaging. *IEEE Access*, 7, 140233–140251. <https://doi.org/10.1109/ACCESS.2019.2932130>
- Wang, Y., Song, W., Fortino, G., Qi, L.-Z., Zhang, W., & Liotta, A. (2019b). An Experimental-Based Review of Image Enhancement and Image Restoration Methods for Underwater Imaging. *IEEE Access*, 7, 140233–140251. <https://doi.org/10.1109/ACCESS.2019.2932130>
- Wu, M., Luo, K., Dang, J., & Li, D. (2017). Underwater image restoration using color correction and non-local prior. *OCEANS 2017 - Aberdeen*, 2017-Octob, 1–5. <https://doi.org/10.1109/OCEANSE.2017.8084916>